



Acute salt stress promotes altered assembly dynamics of nascent freshwater microbial biofilms

Jonathon B. Van Gray · Alescia A. Roberto · Laura G. Leff

Received: 20 August 2019 / Revised: 10 April 2020 / Accepted: 16 April 2020 / Published online: 25 April 2020
© Springer Nature Switzerland AG 2020

Abstract Freshwater ecosystems are under increasing threat of salinization due to human activity. Given the contributions of microbial communities to stream ecosystems, it is critical to understand how these communities are affected by the increasing presence of salt in the environment. We used an artificial stream system to investigate how salt concentrations representing the 95th- and 99th-percentile of concentrations observed in NE Ohio streams affect bacterial community succession and what implications this has on community-level functional capabilities. We hypothesized that the successional trajectory of community functionality (in the form of extracellular enzyme activity) and structure (via denitrification gene abundances and community 16S rRNA gene profiles) would be altered in response to increasing salt concentrations. We observed considerable structural

changes in bacterial composition among treatments that corresponded with niche expansion by more salt-tolerant taxa. Increases in denitrification gene abundances and modifications to extracellular enzyme activity were also observed. These data suggest that continued salt pollution can dramatically affect community structure and has the potential to modify the functional contributions of the bacterial community to the ecosystem.

Keywords Bacterial biofilm succession · Freshwater salinization · Denitrification genes

Introduction

Increasing concentrations of inorganic salts (hereafter salts) in the environment are closely linked to human activity. Salt contributions from point (e.g., waste water treatment plant effluent, etc.) and nonpoint sources, such as road deicing agents (e.g. MgCl, NaCl) in snow-affected areas (Corsi et al., 2015; Roy et al., 2015; Evans et al., 2018), agricultural practices (Williams, 2001), and industrial water uses (e.g. mining and natural gas extraction; Cañedo-Argüelles et al., 2012), have resulted in an increase in the salinization rates of streams globally (Kaushal et al., 2018) as well as the diversity and concentrations of inorganic salts in the environment (Cañedo-Argüelles

Handling editor: Stefano Amalfitano

Electronic supplementary material The online version of this article (<https://doi.org/10.1007/s10750-020-04266-2>) contains supplementary material, which is available to authorized users.

J. B. Van Gray · A. A. Roberto · L. G. Leff
Department of Biological Sciences, Kent State University,
Kent, OH 44242, USA

J. B. Van Gray (✉)
Ohio State ATI, 1328 Dover Road, Wooster,
OH 44691, USA
e-mail: vangray.1@osu.edu

et al., 2016; Hintz & Relyea, 2017; Schuler et al., 2017). When coupled with landscape modifications that increase overland water flow (such as in agricultural [e.g. tile drainage] and urban systems [e.g. expansion of impervious surfaces]), highly soluble salts are readily transported from the site of origin to surface and subsurface waters (Kaushal et al., 2005; Lax & Peterson, 2009). Although dilution and downstream export may occur, elevated salt concentrations can persist in the environment well beyond their initial introduction to the system, thereby increasing background concentrations (Lax & Peterson, 2009; Corsi et al., 2015).

Salt stress can be detrimental to freshwater microbial communities, altering community composition and diminishing critical community and ecosystem-level processes. Increased salinity can dramatically modify aquatic chemistry (Duan & Kaushal, 2015), affecting cation exchange capacity of stream sediments leading to increases in base cations, NH_4^+ (Baldwin et al., 2006), dissolved organic carbon, nitrogen (Duan & Kaushal, 2015), phosphorus (Weston et al., 2006), and metals (Löfgren, 2001; Kim & Koretsky 2013). Subsequent physiological stress caused by osmotic imbalances in ionic concentrations can be detrimental to microbes that lack morphological or physiological adaptations necessary to maintain cellular homeostasis under elevated salinity (Hart et al., 1991; Sleator & Hill, 2002). For bacteria, this often entails energy-intensive accumulation or production of osmolytes within the cell to achieve osmotic equilibrium with the external environment in addition to those required for basal cellular functioning (Oren, 1999; Sleator & Hill, 2002; Sévin et al., 2016). This balancing act between equilibration and cellular functioning can lead to an increased incidence of dormancy or possible extirpation from the local environment (Logares et al., 2009; Aanderud et al., 2016).

Examinations of microbial communities along naturally occurring salinity gradients have observed altered or diminished functional capacity occurring with increasing salinity. For instance, Dupont et al. (2014) identified several core metabolic processes and pathways (via occurrence and frequencies of KEGG functional modules) that appear to diverge along salinity gradients, suggesting that a strong environmental selection for genetic and functional characteristics takes place in response to salinization. In

particular, respiratory and glycolytic pathway specificity (e.g., reliance on the Embden-Meyerhof-Parnas versus the Entner-Doudoroff glycolytic pathways) appear to be closely linked to salinity concentrations, indicating that energy dynamics may be compromised under altered salt concentrations. Moreover, the activity of extracellular enzymes responsible for resource and nutrient acquisition may be negatively affected as priorities shift from enzyme production to osmoregulation, thereby limiting nutrient or C uptake (Rietz & Haynes, 2003; Servais et al., 2019). As a result, modified nutrient acquisition strategies and requirements of salt-affected populations may further disrupt nutrient cycling, thereby extending the impacts of salinity beyond the site of initial impairment. For instance, Wang et al. (2018) identified significant reductions in *nirK* and *nosZ* gene abundances in mangrove sediments that had elevated salinity levels, suggesting that the denitrifier community and corresponding functional potential is likely affected by strong environmental selection. In addition, a number of functional attributes of communities, such as denitrification (Weston et al., 2006; Franklin et al., 2017), methanogenesis (Osaka et al., 2008), bacterial productivity, and respiration (Dupont et al., 2014), and extracellular enzyme activity (Reed and Martiny, 2013) are negatively affected by increasing salinity, indicating that both potential (e.g. KEGG profiles and denitrification gene abundances) and realized (e.g. N reduction, C oxidation, etc.) community contributions to ecosystem function are affected. While these results may be attributable to physiological constraints under saline stress, it may also reflect increased bacterial dormancy as a means of weathering an inhospitable environment (Logares et al., 2009; Aanderud et al., 2016).

Patterns in bacterial phylogenetic diversity have also been closely linked to salinity, indicating strong environmental selection for lineages capable of withstanding elevated saline conditions (Lozupone & Knight, 2007). Likewise, along the salinity gradient of estuaries, there are phylum-level compositional shifts (from Betaproteobacteria and Actinobacteria to α -Proteobacteria dominated communities) with increasing salinity (Bouvier & del Giorgio, 2002; Fortunato et al., 2011; Telesh & Khlebovich, 2010; Campbell & Kirchman, 2012). Similar high-level taxonomic responses have been observed in reciprocally transplanted wetland communities from low- and

high-salinity environments (Morrissey & Franklin, 2015). These patterns suggest that the divergence in salinity preferences occurred early in bacterial evolutionary history and that despite the presence of halotolerant lineages within many phyla, indigenous freshwater or marine clusters are likely to have arisen that have remained relatively isolated due to a saline-induced marine-freshwater colonization barrier (Zwart et al., 2002; Logares et al., 2009; Morrissey & Franklin, 2015).

The potential impact of salinization on freshwater microbial communities has not been widely considered despite continued freshwater salinization (Kaushal et al., 2018). As a result, many of the inferences made about freshwater community response are based on data from naturally occurring salinity gradients (i.e., in estuaries) and may have little bearing on freshwater ecosystems. Specifically, halotolerant taxa are likely present along natural salinity gradients due to the proximity to saline environments (Campbell & Kirchman, 2012; Dupont et al., 2014); thus, it is important to consider the effects of salinization on freshwater communities where halotolerant populations may not be present or may be present in reduced quantities. Furthermore, the response of these communities to elevated salinity during the early stages of community assembly has not been established despite the implications for community development. This early phase of colonization is especially significant as the order in which individuals arrive influences assembly trajectories (via priority effects or niche differentiation; Samuels & Drake 1997; Fukami & Wardle, 2005; Lear et al., 2012), thereby affecting patterns of community composition and functional diversity (Tolker-Nielsen & Molin, 2000; Ren et al., 2018). Moreover, many of the bacterial taxa (e.g. β -Proteobacteria) responsible for ecologically relevant processes, such as denitrification, may be established early during succession (Manz et al., 1999; Araya et al., 2006) as anoxic microenvironments are created during biofilm biomass accrual (Stoodley et al., 2002; Lawrence et al., 2007)—a process that may be inhibited by osmotic stress (Bazire et al., 2007; Katebian & Jiang, 2013; Kim & Chong, 2017).

To address these unknowns, controlled laboratory experiments were carried out using recirculating flume microcosms to examine bacterial community assembly dynamics during early colonization under the

stress of freshwater salinization. We hypothesized that salinization (as represented by the sum of total dissolved solids within the stream/flume water; hereafter TDS [CWT, 2004]) would affect both the function and structure of the bacterial community. First, we hypothesized there would be reduced extracellular enzyme activity (EEA) associated with elevated TDS (H1). We predicted that this would alter both individual EEA as well as EEA ratios, thus providing insights into the general resource requirement of the affected communities. Quantities of genes associated with denitrification (specifically those associated with nitrite [*nirS*] and nitrous oxide [*nosZ*] reduction) were also hypothesized to decrease as a function of TDS concentrations (H2). Although denitrification is typically associated with anaerobic environments, many bacterial populations responsible for ecologically relevant processes (e.g. β -Proteobacteria) become established early during succession (Manz et al., 1999; Araya et al., 2006). This is likely in part due to their metabolic plasticity which may permit transitions from aerobic to anaerobic lifestyles (Robertson & Kuenen, 1984; Arnon et al., 2007; Lycus et al., 2018), but also as the result of anoxic microenvironments developing within biofilms as biomass accrues (Stoodley et al., 2002; Lawrence et al., 2007). We predicted that a reduction in denitrification gene abundance would likely reflect the decreased denitrification often observed under saline stress (Irshad et al., 2005; Rath et al., 2016) or the inhibitory effects of elevated salinity on biofilm biomass accrual (Bazire et al., 2007; Katebian & Jiang, 2013; Kim & Chong, 2017). Finally, we hypothesized that alterations in community composition would occur such that taxa capable of tolerating elevated salinity become more prevalent while more sensitive taxa are extirpated (H3) as conditions are likely to exceed the functional operational range (Hallin et al., 2012) typically experienced by colonizers under ambient conditions. We predicted this would result in reduced α -diversity with increasing TDS concentrations and that communities would become increasingly dissimilar (as characterized by β -diversity) with increasing salinity. Taxa present in all samples were considered to be tolerant to the ranges of salinity examined here, while taxa absent from either the controls or the highest TDS flumes were assumed to be obligate freshwater or saline, respectively.

Materials and methods

Nine recirculating laboratory flumes were constructed with three replicates per treatment run simultaneously. The flume design was chosen because of its ability to reproduce unidirectional flow patterns similar to those found in lotic systems and reproducibility of results (Singer et al., 2006; Besemer et al., 2007). Further, this design simulates a stable hydrologic state while being able to maintain control of the community and environmental conditions, which is not possible in environmental studies.

Flumes were constructed from 1.3 m lengths of 30.8 mm × 76.2 mm vinyl rain downspouts, of which one 1.3 m × 76.2 mm side was removed to create an open channel with a total possible volume of 3 l. Three 18.93 l buckets were acid-washed and cleaned with 10% bleach solution before being used as treatment-specific feeder/collection tanks that were shared among the three replicates (Supplemental Figure 1). For each treatment, water was pumped from a feeder tank using a Sicce Syncra Silent 3 Multifunction Aquarium pump into each of the replicate flumes and effluent was collected in treatment-specific tanks before being recirculated back into the flumes. A portable water flow meter was used to establish mean flume water velocity of approximately 0.1625 m s^{-1} (Marsh/McBirney Electromagnetic Flow Meter model 201). Each flume contained two rows of $52 \times 2.54 \text{ cm}^2$ ceramic tiles that had been baked in a muffle furnace at 500°C for 4 h and then autoclaved prior to placement. Tiles within the first and last 10 cm of the flume were not disturbed over the course of the experiment as a means of normalizing flow patterns upstream and downstream of the sampling area. Each set of flumes was equipped with a 1.22-m linear light containing two GE 32 W 6500 K Natural Daylight Fluorescent bulbs which were set to a 12-h:12-h light:dark cycle.

Experimental design

To select an appropriate range of treatment concentrations, water quality data from the Erie/Ontario Drift and Lake Plain Level III Ecoregion of Ohio (Omernik, 1987), with Lake Erie serving as the northernmost boundary and 82° W longitude as the westernmost boundary, were obtained from the Water Quality Portal database (<https://www.waterqualitydata.us>;

accessed 09/12/16). Due to the vast number of potential chemical constituents contributing to environmental TDS, Cl^- was chosen as a proxy for TDS for the purpose of manipulating water quality in the laboratory and was significantly correlated with TDS in the regional data ($P < 0.05$, $r = 0.84$). Summary statistics were calculated for Cl^- concentrations and two treatment values were chosen that were representative of the 95th (306.5 mg l^{-1}), and 99th (1650 mg l^{-1}) percentiles from the region.

The experiment was run 3 times, with each iteration lasting a total of 9 days. At the start of each iteration (day 0—09/23/2016, 10/03/2016, and 10/12/2016), water and microbial communities were collected from a 5th-order reach (Strahler, 1964; Peck, 2012) of the Cuyahoga River at Waterworks Park in Munroe Falls, OH, a developed/suburban area within the larger Akron Metropolitan area and located in the temperate Erie/Ontario Drift and Lake Plain ecoregion of northeast Ohio. Previous assessments of macroinvertebrate communities from this reach suggest it is of relatively high-quality and thus suitable for this study. Additional water was collected from the Cuyahoga River site to replace the header tank water on day 4 of each experiment to ensure adequate nutrients were available for community development and to account for any shifts in composition of the pool of potential colonizers. Mean historical Cl^- concentration (89.3 mg l^{-1}) was used as the baseline condition for the duration of this study. Water samples were collected and placed on ice for transport back to the laboratory.

Upon returning to the laboratory, water samples were combined and thoroughly mixed to minimize the heterogeneity of the community. Equivolumes of water (15 l) were distributed among the header tanks of each set of experimental flumes. Flumes were assigned to either control or treatment groups, and treatment groups were amended with NaCl so that the final Cl^- concentrations of the water in all three header tanks were representative of baseline (89.3 mg l^{-1} ; hereafter the control), 95th (306.5 mg l^{-1} ; hereafter the 95% treatment), or 99th (1650 mg l^{-1} ; hereafter the 99% treatment) percentile conditions. On day 4 water in the tanks was replaced with additional water (as previously discussed) and once again amended with Cl^- so as to establish previous treatment concentrations.

Sample collection and analysis

Environmental conditions, including dissolved oxygen (DO), conductivity (normalized for temperature), pH, redox potential, and temperature, were measured at days 0 and 4 (Table 1) for each treatment using a handheld Hach HQ40d multiprobe unit (Hach, Loveland, CO, USA). Over the course of each experiment, water samples were collected from each flume at 2-day intervals on days 1, 3, 5, 7, and 9 to determine nutrient (NO_3^- and NH_4^+) concentrations and TDS. Nutrient concentrations were determined using the 96-well plate method (Ringuelet et al., 2011) and quantified on a Synergy 4 microplate reader (BioTek, Winooski, VT, USA) at 540 and 630 nm for NO_3^- and NH_4^+ , respectively. TDS was determined by filtering 100 ml of water through 47 mm 1.5 μm Whatman glass fiber filters (GE Healthcare Biosciences, Pittsburgh, PA, USA) in triplicate and filtrate was weighed and evaporated in a drying oven at 180°C for 2 h. Once cooled to room temperature, dried samples were weighed, and TDS was calculated as dry sample weight (sans evaporation dish) per original sample volume (mg l^{-1}).

Randomly selected tiles ($n = 10$) from each flume were collected and replaced with acid-washed and autoclaved tiles at 2-day intervals over the course of 9-day colonization period. This duration was chosen to approximate the time period in which the greatest decline in the rate of new bacterial taxa contributing to overall biofilm richness occurs (Jackson, 2003), thus increasing the likelihood that the populations present will play a role in biofilm maturation. Biofilms from tiles of individual flumes were collected and pooled for a total of 3 replicates per sample time per

treatment. DNA was extracted using Mo-Bio Power-soil DNA Isolation kits (Mo-Bio, Carlsbad, CA, USA) per the manufacturer's instructions and quantified via fluorometrically using Invitrogen Quant-iT PicoGreen reagent on a Synergy 4 microplate reader (BioTek, Winooski, VT, USA). Despite the known biases introduced during PCR being exacerbated by employing nested PCR, low biomass accrual during early stages (days 1 and 3) of biofilm development necessitated that PCR amplification of 16S rRNA genes was performed prior to samples being sent for sequencing. PCRs included 2 μl of 5 $\mu\text{g l}^{-1}$ sample DNA, 7 μl molecular grade H_2O , 15 μl Promega Master Mix 2 \times (50 U ml^{-1} Taq DNA polymerase in proprietary reaction buffer, 400 μM of each dNTP, 3 mM MgCl_2 ; Madison, WI, USA), 3 μl of 0.4 $\mu\text{g l}^{-1}$ bovine serum albumin (Promega, Madison, WI, USA), 1.5 μl each of 10 μM forward primer 357F (5'-CTCCTACGG-GAGGCAGCAG-3'; Turner et al., 1999) and reverse primer 1391R (5'-GACGGCGGTGTGTRCA-3'; Turner et al., 1999). PCR conditions consisted of 3-min denaturation at 95°C followed by 35 cycles (94°C for 30 s, 58°C for 30 s for annealing, 72°C for 90 s) and a final extension for 7 min at 72°C. PCR products from each sample were normalized to 25 ng DNA μl^{-1} and sent to The Ohio State University's Molecular and Cellular Imaging Center (MCIC) for paired-end sequencing of the V4 region (forward primer 515F, 5'-GTGCCAGCMGCCGCGGTAA-3' and reverse primer 806R, 5'GGACTACHVGGGTWTCTAAT-3'; (Caporaso et al., 2012) of the 16S rRNA gene using the Illumina MiSeq platform. Samples were demultiplexed by MCIC staff prior to further analysis. Raw sequence data was deposited in the Sequence Read Archive of

Table 1 Flume environmental conditions

Treatment	Sample time	Conductivity $\mu\text{S cm}^{-1}$	Temperature (°C)	Redox potential (mV)	pH
Control	Day 0	598 (104)	20.4 (1)	354.6 (105.8)	8.21 (0.26)
95%	Day 0	1033 (137)	19.9 (1)	335.2 (91.5)	8.29 (0.28)
99%	Day 0	3320 (582)	20.3 (1)	422 (235.3)	8.29 (0.26)
Control	Day 4	834 (303)	20.3 (1)	272.0 (60.2)	8.22 (0.13)
95%	Day 4	1078 (42)	19.8 (0.1)	295.3 (33.6)	8.33 (0.1)
99%	Day 4	3587 (110)	20.2 (0.3)	290.3 (22.1)	8.36 (0.08)

Mean (standard deviation) flume water physicochemical parameters measured at the start (Day 0) and refresh date (Day 4) for each iteration of the experiment

the National Center for Biotechnology Information under the identifier SUB6189612.

Sequence data was processed through the QIIME 2 (version 2017.10) bioinformatics pipeline (www.qiime2.org; Caporaso et al., 2010) to assess data quality, remove spurious sequences, and to assign taxonomy. In brief, sequences were trimmed to 230 bp to maintain a median Q30 Phred score, representing a 99.9% base call accuracy. The DADA2 algorithm (Callahan et al., 2016) was applied to the remaining sequences to correct Illumina-induced amplicon errors. A Naïve Bayes classifier (Zhang, 2004) was trained on the GreenGenes database (version 13_8; 97% sequence similarity resolution) before being applied to sample sequence classification. Mitochondrial, chloroplast, and singleton sequences were removed. Samples were then rarefied to a depth of 3089 sequences—resulting in the retention of 115 samples and 40.11% of sequences. These data were used to calculate α -diversity indices (Shannon diversity index, inverse Simpson's index, Pielou's evenness, and OTU richness) and β -diversity via Bray-Curtis dissimilarities using the R statistical environment (v3.3.1; R Core Team, 2016). Sequences were then aligned using the MAFFT sequence alignment program (Katoh et al., 2002) and unrooted phylogenetic trees were inferred using FastTree v2.1 (Price et al., 2009), each within the QIIME2 framework. Additional α -diversity (Faith's PD) and β -diversity (weighted and unweighted UniFrac distances) estimates were calculated in QIIME2 and exported for use in R.

Quantitative-PCR (qPCR) was used to quantify *nirS* and *nosZ* gene abundance under varying TDS concentrations. Reactions consisted of 2 μ l of 5 μ g μ l⁻¹ sample DNA, 10 μ l of 1 \times PerfeCTa SYBR Green SuperMix reaction buffer (consisting of a proprietary mix of MgCl, dNTPs, AccuStart II Taq polymerase, SYBR Green I dye, and enzymatic stabilizers and additives; QuantaBio, Beverly, MA, USA), 6.2 or 7.2 μ l molecular grade H₂O (for *nirS* and *nosZ* amplification, respectively), and 0.8 (*nirS*) or 0.4 (*nosZ*) μ l each of 10 μ M forward (*nirS*3Fa: 5'-TTCCT(T/C/G)CA(C/T)GACGG(C/T)GG-3', Throbäck et al., 2004); *nosZ*-F: 5'-CG(C/T)TGTT(C/A/C)TCGACAGCCAG-3', (Kloos et al., 2001) and reverse (R3cd: 5'-GA(C/G)TTCGG(A/G)TG(C/G)GTCTTGA-3', Throbäck et al., 2004; *nosZ*1622R: 5'-CGC(G/A)A(C/G)GGCAA(G/C)AAGGT(G/

C)CG-3', Throbäck et al., 2004) primers. Reactions targeting *nirS* abundances also contained 0.2 μ l of 0.4 μ g μ l⁻¹ bovine serum albumin (Promega, Madison, WI, USA). Conditions for *nirS* analysis consisted of an initial step at 95°C for 3 min, followed by 40 cycles (95°C for 1 min, 56°C for 1 min, and 72°C for 1 min), and completing with a melting curve cycle consisting of 95°C for 15 s, 60°C for 15 s, and 95°C for 15 s. Conditions for *nosZ* PCR consisted of an initial step at 95°C for 3 min, followed by 40 cycles (95°C for 30 s, 56°C for 30 s, and 72°C for 30 s), and completing with a melting curve cycle consisting of 95°C for 15 s, 60°C for 15 s, and 95°C for 15 s.

Due to the limited biomass accrual on tiles, water samples were collected from each set of flumes at day 1, 3, 5, 7, and 9 and used to quantify extracellular enzyme activities (EEAs). Briefly, 100 μ l of sample water was placed in Costar 96-well black polystyrene plates with 100 μ l of 300 μ M fluorogenic 4-methylumbelliferone (MUB) labeled β -glucosidase (BGLU), β -xylosidase (BXYL), and phosphatase (PHOS), or 7-amino-4-methylcoumarin (AMC) labeled leucine aminopeptidase (LAP) enzyme substrates. Additional wells containing sample water, MUB or AMC, and MUB or AMC-labeled enzyme substrates were included as blanks and controls to account for extraneous fluorescence. Plates were incubated in the dark at room temperature for 40 min. Sample fluorescence was read at 360 nm and 460 nm (excitation and emission, respectively) on a BioTek Gen5 plate reader and software (Winooski, VT, USA; modified from DeForest, 2009; Smucker et al., 2009). EEA was calculated using modified equations from Smucker et al. (2009). In addition, vector lengths and angles were calculated from the proportional activity of C acquisition EEA to nutrient acquisition EEA (Moorhead et al., 2016):

Vector length

$$= \sqrt{\left(\frac{[\text{BGLU} + \text{BXYL}]}{[\text{LAP}]}\right)^2 + \left(\frac{[\text{BGLU} + \text{BXYL}]}{[\text{PHOS}]}\right)^2}$$

In this context, vector length corresponds to relative C-to-nutrient limitation (e.g. longer vectors equate with higher C:nutrient ratios) while the vector angle quantifies P-to-N limitation (e.g. where angles correspond with increasing P limitation $< 45^\circ <$ increasing N limitation) and permits for the exploration of

coupled C, N, and P dynamics as a function of treatment and sampling day (Moorhead et al., 2016):

$$\text{Vector angle(degrees)} = \tan^{-1} \left(\frac{\text{BGLU} + \text{BXYL}}{\text{LAP}} + \frac{\text{BGLU} + \text{BXYL}}{\text{LAP}} \right) \times \frac{180}{\pi}$$

Statistical analysis

All statistical analyses were run within the R statistical environment (v3.3.1; R Core Team 2016). Analyses of covariance (ANCOVAs; for data from flume water, with sample day as covariate) and repeated measures analyses of variance (ANOVAs; for data from biofilms) were run as linear mixed-effects models (nlme package v3.1-131; Pinheiro et al., 2017).

Linear mixed-effects models were used as they permit inclusion of random effects that can address flume-specific flow heterogeneity, account for temporally-induced variations stemming from multiple iterations of the experiment being run, and as a means of implementing appropriate variance structures to diminish heteroscedasticity when necessary. Two different types of models were selected due to the potential for the flume water replenishment to artificially influence the results. Sampling day was included in biofilm-specific data analysis due to the cumulative characteristics of a developing biofilm community relative to the transience of the overlying water. All models were examined for assumptions of normality; response data was standardized by treatment type, sampling day, and treatment-day interaction and data points ± 2 standard deviations from the mean were considered to be outliers and removed unless determined to be biologically relevant. Variables including *nosZ* and *nirS* abundances, and Faith's phylogenetic diversity data were log-transformed prior to analysis. Data that continuously failed to meet the assumptions required for parametric tests (e.g. Pielou's evenness, Shannon diversity index, inverse Simpson's diversity index) were analyzed first using a Kruskal–Wallis rank sum test with treatment \times sampling day interactions and if no significant differences were observed, a Kruskal–Wallis test was used to examine treatment effects.

Post hoc analyses were carried out on models in which treatments or treatment-sampling day

interactions were significant. Benjamini-Hochberg corrected multiple comparisons (Benjamini & Hochberg, 1995) were performed using the `glht` function in the `multcomp` package (Hothorn et al., 2008) in conjunction with the `lsm` function in the `lsmeans` package (Lenth, 2016) in order to identify significant differences between specific treatments or specific treatment-sample time interactions.

Bray–Curtis (B–C) dissimilarities derived from Hellinger-transformed, family-level taxonomic community data as well as weighted (based on relative abundance data) and unweighted (based on presence-absence data) Uni-Frac distances were used in principle coordinates analysis to visualize community composition in ordination space. These data were used in permutational analysis of multivariate homogeneity of group dispersions (PERMDISP2; Anderson et al., 2006) and permutational multivariate analysis of variance (PERMANOVA; Anderson, 2001) as a means of assessing the effects of treatment and sampling day on β -diversity. PERMDISP2 were employed to compare the homogeneity of community dispersion as an interactive effect of treatment and sampling day using the `betadisper` function in the `vegan` package. PERMANOVAs were performed with the `adonis2` function in the `vegan` package (v2.4-5, Oksanen et al., 2016) to compare the central tendency of each community to treatment and sampling time. Permutations were restricted to each iteration of the experiment in an attempt to minimize any temporally-induced compositional variability. If no significant treatment \times time interactions occurred, analyses were re-run solely examining the effects of treatment. Multiple comparisons among and between treatments at each sampling time were also performed using the `adonis2` function and the Benjamini–Hocheberg procedure was implemented to control the false discovery rate of resulting p-values. Similarity percentage of discriminating OTUs (`simper`; Clarke, 1993) between communities were assessed using the `simper` function in the `vegan` package to elucidate compositional changes in the community and to identify which OTUs were significantly affecting the observed changes between the 95% and 99% treatments and the control. Spearman's rank correlations will be used to further explore the response (+ or –) of these discriminating OTUs to TDS concentrations.

Results

Despite the temporal nature of the experiments, no significant temporal effects were observed; however, several salt-treatment effects were observed, and data is presented so as to highlight these differences. Significantly different TDS concentrations among the three treatments (e.g. control, 95% and 99%) were maintained throughout the experiment (Fig. 1A). Ammonium concentrations (Fig. 1B) significantly decreased with increasing TDS, falling from a mean concentration of 0.157 mg l^{-1} in the control to

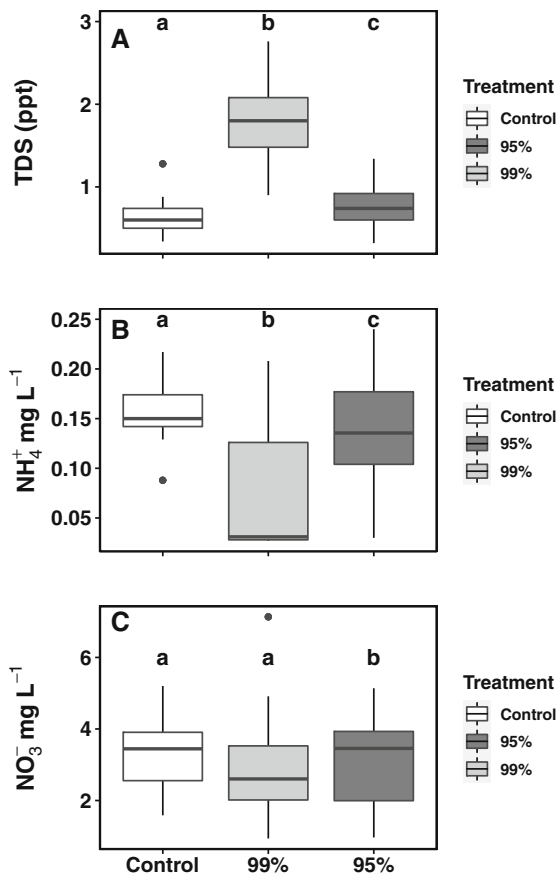


Fig. 1 Total dissolved solids and nitrogen concentrations. Box and whisker pots of total dissolved solids (TDS; **A**), NH_4^+ (**B**), and NO_3^- (**C**) concentrations in each treatment. Horizontal bar represents median value of sample, box represents the interquartile range (IQR) and whiskers represent $1.5 \times \text{IQR}$. Data points falling outside of the whiskers represent outliers in untransformed data. Letters directly above boxplots indicate whether or not significant (letters differ) or no significant (letters are the same) differences were observed among treatments

0.137 mg l^{-1} and 0.075 mg l^{-1} in the 95% and 99% treatments, respectively. Nitrate concentrations (Fig. 1C) were not significantly different between the control and 95% treatments (mean: 3.26 mg l^{-1} and 3.07 mg l^{-1} , respectively), while the 99% treatment resulted in a significant decrease (mean: 2.99 mg l^{-1}).

Patterns of difference among treatments in EEA varied among individual enzymes. Activity of BGLU, an enzyme associated with C-acquisition via cellulose hydrolysis (Fig. 2A) was not affected by treatments, while BXYL activity increased with treatment intensity (mean: 0.58 , 0.66 , and $0.72 \text{ nmol h}^{-1} \text{ cm}^{-2}$ for the control, 95% and 99% treatments, respectively), indicating additional xylose degradation potential occurred in elevated saline treatments (Fig. 2B).

Nutrient scavenging enzyme activity exhibited significant treatment effects; the direction of the response differed between enzymes associated with N- and P-acquisition. A significant decline was observed in LAP activity (N acquisition) with increasing treatment intensity (mean: 3.73 , 3.68 , and $3.64 \text{ nmol h}^{-1} \text{ cm}^{-2}$ for the control, 95% and 99% treatments, respectively; Fig. 2C). Conversely, PHOS activity—a proxy for P requirements—remained lower in the control treatment relative to the saline amended flumes (mean: 6.38 , 6.81 , and $6.84 \text{ nmol h}^{-1} \text{ cm}^{-2}$ for the control, 95% and 99% treatments, respectively; Fig. 2D), indicating potential P deficiency within communities experiencing elevated salinity.

Vector analysis of enzyme ratios provides context for individual enzyme activities and insights into resource requirements of the community (Moorhead et al., 2016). Analysis of EEA-derived vector lengths identified significantly increased C:nutrient EEA ratios in the saline treatments (Supplemental Fig. 2A), indicating increased enzymatic activity related to C acquisition relative to nutrient acquisition. This coincided with a decrease in vector angle within the saline treated flumes (Supplemental Fig 2B), suggesting that these treatments were trending towards a more P-limited state (Fig. 3).

Abundances of the two targeted N-cycling genes (*nirS* and *nosZ*) genes varied in their response to treatment; *nirS* abundance was unaffected by treatment (mean: 2.86×10^7 *nirS* copies across all groups; Fig. 4A) while a significant increase in *nosZ* abundance was observed in both the 95% (mean 2.08×10^6

Fig. 2 Extracellular enzyme activity under salt stress. Box and whisker plots of individual extracellular enzyme activities for C-acquiring enzymes BGLU (A) and BXYL (B), N-acquiring enzyme LAP (C), and P-acquiring enzyme PHOS (D) in each treatment. Horizontal bar represents median value of sample, box represents the interquartile range (IQR) and whiskers represent $1.5 \times$ IQR. Data points falling outside of the whiskers represent outliers in untransformed data. Letters directly above boxplots indicate whether or not significant (letters differ) or no significant (letters are the same) differences were observed among treatments

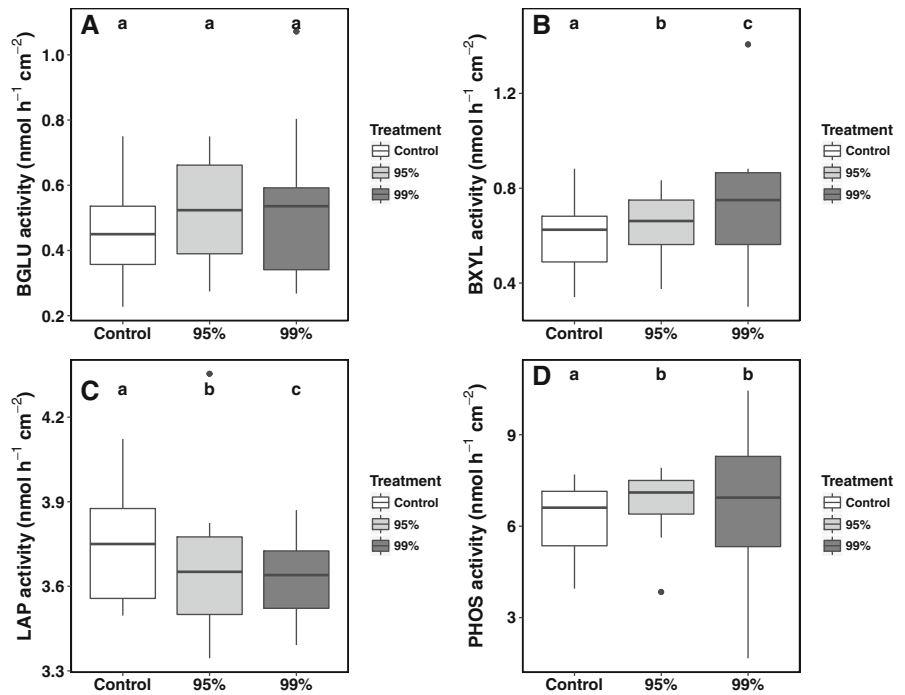
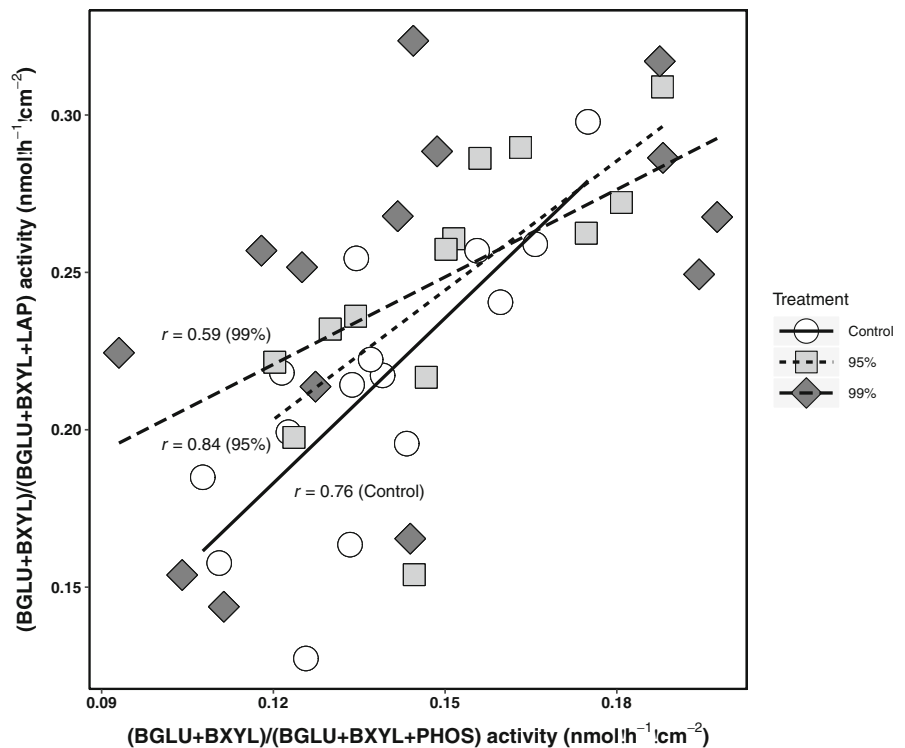


Fig. 3 C/C + N to C/C + P EEA ratios. Scatterplot of C:C + N (y-axis) and C:C + P (x-axis) EEA ratios. Point shapes represent individual treatments (circle = Control, triangle = 95%, and square = 99%). Correlation coefficients and trendlines for each treatment (solid = Control, dotted = 95%, and dashed = 99%) included to visualize general trends in nutrient limitation



copies; Fig. 4B) and 99% (mean: 7.60×10^6 copies; Fig. 4B) treatment groups relative to the controls (mean: 2.05×10^6 copies; Fig. 4B).

Significant treatment differences were observed for both OTU richness and Faith's pd (Fig. 5A, B). Family-level OTU richness was higher in the 95%

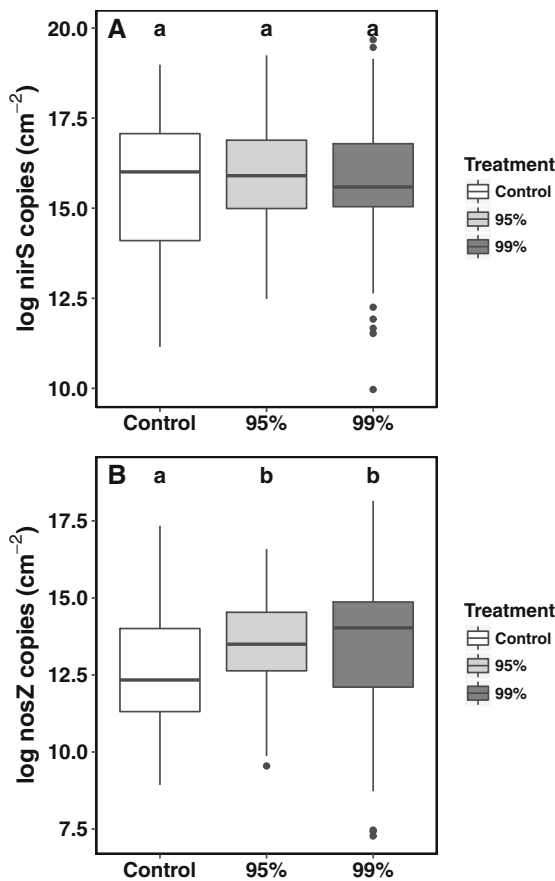


Fig. 4 Denitrification gene abundances under salt stress. Box and whisker plots of log-transformed abundances of *nirS* (A) and *nosZ* (B) copy numbers in each treatment. Horizontal bar represents median value of sample, box represents the interquartile range (IQR) and whiskers represent $1.5 \times$ IQR. Data points falling outside of the whiskers represent outliers in untransformed data. Letters directly above boxplots indicate whether or not significant (letters differ) or no significant (letters are the same) differences were observed among treatments

treatments than in the control (mean: 50) and 99% (mean: 49) treatment. Faith's pd, a phylogenetically-derived analog of OTU richness, was significantly lower in the 99% treatment (mean: 4.4) relative to the control (mean: 5.3) and 95% treatments (mean: 5.4). None of the other 3 metrics examined (Pielou's evenness, Shannon diversity index, or the inverse Simpson's index Fig. 5C–E, respectively) exhibited any significant differences among treatments.

Multivariate analysis of the community variance revealed no significant differences among treatment groups, indicating homoscedasticity between groups regardless of distance method used and validating

PERMANOVAs as an appropriate assessment method. Multivariate analyses (PERMANOVAs) of community profiles identified significant ($P < 0.05$) shifts in community composition with treatment. B-C dissimilarities demonstrated significant differences among in community composition among all treatment groups (Fig. 6A). UniFrac distances identified significant compositional differences between the control and 99% treatments (weighted UniFrac; Fig. 6B) and between the control and both the 95% and 99% treatments (unweighted UniFrac; Fig. 6C). Although no significant treatment-sampling time interactions were observed, sampling time did significantly affect community trajectory and exhibited similar patterns across all treatments in ordination space.

Examination of treatment-discriminating taxa, as determined by simpler analysis, identified 40 family-level OTUs that significantly affected shifts in community composition; of these only 13 were correlated with TDS concentrations ($P < 0.05$; Table 2). However, these 13 OTUs represented $> 40\%$ of the total communities (e.g., control, 95% and 99%) examined. For the majority of these OTUs, an increase in treatment intensity corresponded with decreasing relative abundance. In particular, OTUs from the phylum Chloroflexi (Class Ellin6529) and Protobacteria Class Gammaproteobacteria (Order Methylococcales Family Methylococcaceae) were not observed in either of the experimental treatment groups, while OTUs from the Family Sphingobacteriaceae (Phylum Bacteroidetes) were absent from the 99% treatment, only. Conversely, only two OTUs were identified that positively correlated with treatment intensity, including the α -Proteobacteria Order BD7-3 ($\rho = 0.22$, $P = 0.02$) and the γ -Proteobacteria Family Pseudomonadaceae ($\rho = 0.4$, $P < 0.001$).

Discussion

Freshwater salinization is predicted to continue to increase as water use and landscape modifications alter stream environments (Kaushal et al., 2018). Salinization of freshwater can have far-reaching effects on the ecosystem, including alteration to the chemical environment (e.g., cation exchange capacity, metal availability, C and nutrient availability; Baldwin et al., 2006; Weston et al., 2006; Kim & Koretsky,

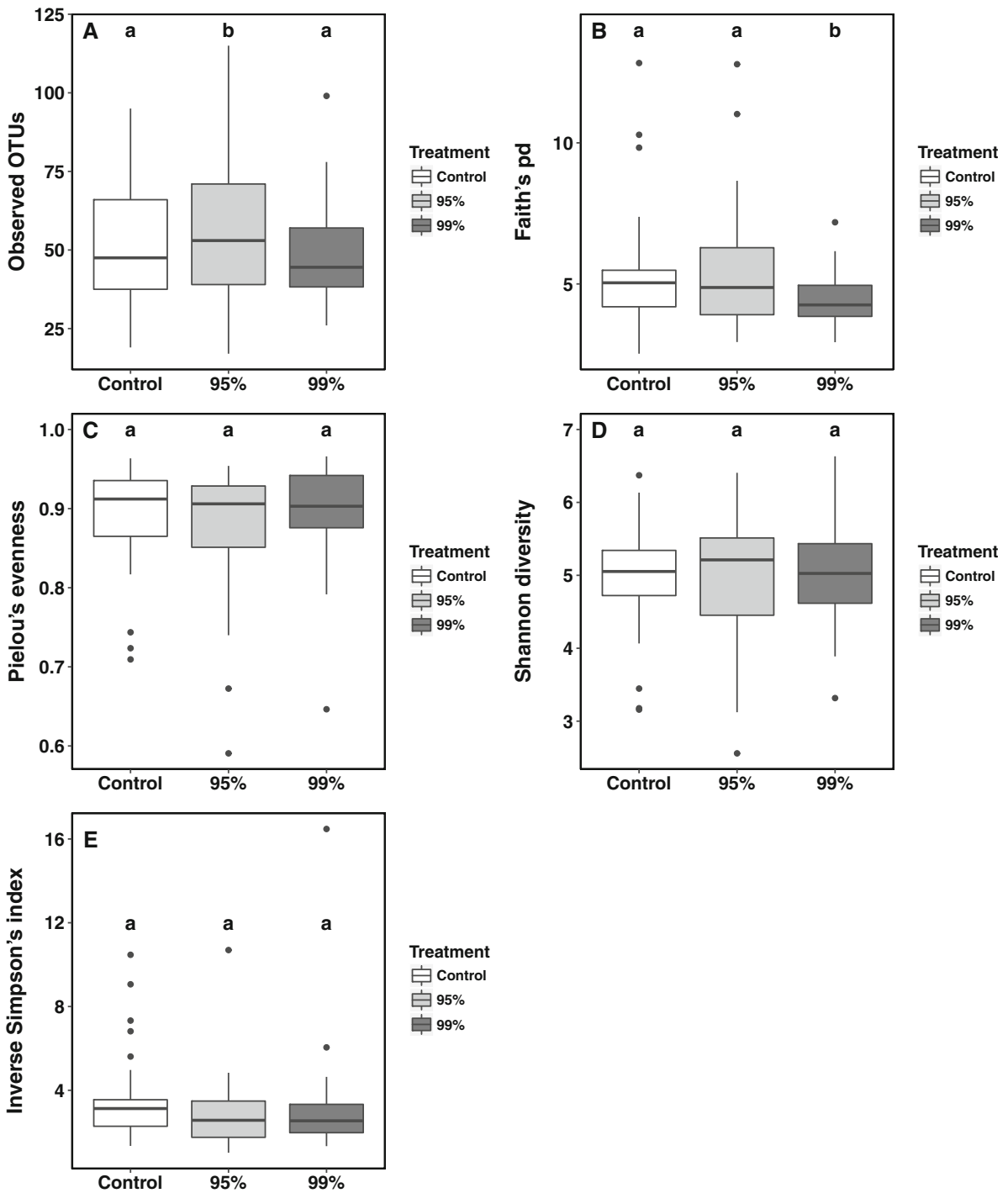


Fig. 5 Alpha diversity under salt stress. Box and whisker plots of several α -diversity metrics including OTU richness (A), Faith's phylogenetic distance (pd) (B), Pielou's evenness (C), Shannon diversity (D), and inverse Simpson's index (E). Horizontal bar represents median value of sample, box represents the interquartile range (IQR) and whiskers represent

$1.5 \times$ IQR. Data points falling outside of the whiskers represent outliers in untransformed data. Letters directly above boxplots indicate whether or not significant (letters differ) or no significant (letters are the same) differences were observed among treatments

Fig. 6 Beta diversity under salt stress. Ordinations of principle coordinates analyses of family-level community data using Bray–Curtis dissimilarities (A) as well as weighted (B) and unweighted UniFrac distances (C) and unweighted UniFrac distances. Point shape represents treatment (circle = Control, triangle = 95%, and square = 99%). Numbers within each shape indicate the sampling time corresponding with that particular community data point. Lines (solid = Control, dotted = 95%, and dashed = 99%) are included to aid in visualization of community trajectory over the course of the study

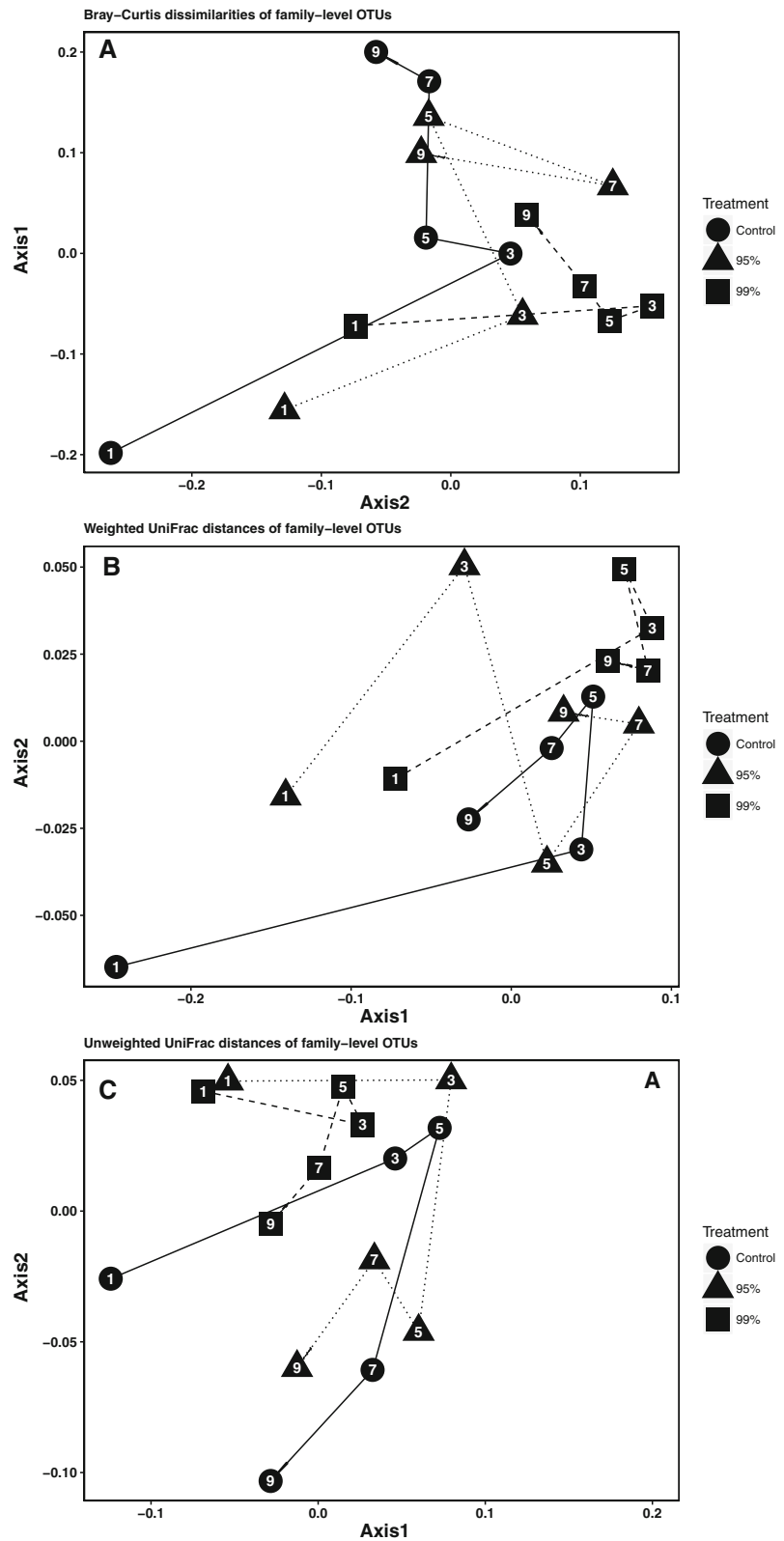


Table 2 Relative abundance of family-level bacterial OTUs

Phylum	Class	Order	Family	Relative abundance— control	Relative abundance— 95%	Relative abundance— 99%
Actinobacteria	Actinobacteria	Actinomycetales	ACK-MI	2.13×10^{-2}	6.74×10^{-3}	3.10×10^{-3}
	[Saprosirae]	[Saprosirales]	Chitinophagaceae	2.69×10^{-3}	1.15×10^{-3}	1.13×10^{-3}
Bacteroidetes	Sphingobacteria	Sphingobacteriales	Sphingobacteriaceae	3.88×10^{-5}	5.96×10^{-5}	0
	OPB56	—	—	2.92×10^{-4}	5.00×10^{-4}	5.49×10^{-5}
Chloroflexi	Ellin6529	—	—	3.61×10^{-4}	0	0
Cyanobacteria	Oscillatoriothycideae	Oscillatoriales	Phormidiaceae	5.63×10^{-3}	4.78×10^{-3}	1.76×10^{-3}
Proteobacteria	Alphaproteobacteria	BD7-3	—	0	3.44×10^{-4}	5.11×10^{-4}
	Betaproteobacteria	Neisseriales	Neisseriaceae	1.94×10^{-2}	5.47×10^{-3}	6.88×10^{-4}
Gammaproteobacteria	Burkholderiales	Burkholderiales	Comamonadaceae	3.15×10^{-1}	2.28×10^{-1}	9.52×10^{-2}
	Pseudomonadales	Pseudomonadales	Pseudomonadaceae	8.01×10^{-2}	1.74×10^{-1}	3.37×10^{-1}
Verrucomicrobia	Methylococcales	Methylococcales	Methylococcaceae	4.58×10^{-4}	0	0
	Xanthomonadales	Xanthomonadales	Xanthomonadaceae	7.49×10^{-3}	2.78×10^{-3}	6.42×10^{-4}
[Spartobacteria]	[Chthoniobacterales]	[Chthoniobacterales]	[Chthoniobacteraceae]	9.23×10^{-4}	1.12×10^{-3}	1.14×10^{-5}

Phylum	ρ	P value	Change from control to 95%	Change from control to 99%	Change of 95% from 99%	Ecological significance
Actinobacteria	-0.36	<0.001	-68.41%	-85.49%	-54.07%	Generally anaerobic; some resistance to antibiotics (Goodfellow 2015)
Bacteroidetes	-0.28	<0.001	-57.16%	-58.03%	-2.03%	Aerobes or facultative anaerobes. Some chitin degraders and some able to hydrolyse cellulose (Rosenberg 2014)
Chloroflexi	-0.2	0.03	53.83%	-100.00%	-100.00%	Strict aerobes. Free-living and saprophytic, although some opportunistic pathogens (The Editorial Board 2015)
Chlorobacteria	-0.24	0.01	71.11%	-81.22%	-89.02%	Sequence originally identified in Obsidian Pool, a hot spring in Yellowstone National Park (Hugenholtz et al., 1997). Likely heterotrophic, relying on small organic molecules, and present across a wide thermal gradient (Hiras et al., 2016)
Chloroflexi	-0.18	0.05	-100.00%	-100.00%	N/A	Diverse metabolic strategies including aerobic and anaerobic strategies, phototrophy and organohalide respiration (Krzmarzick 2012)
Cyanobacteria	-0.26	0.01	-15.09%	-68.76%	-63.21%	Some bloom formation (<i>Planktolithrix</i> , <i>Phormidium</i> , etc.; Heath et al., 2016, Pancrace et al., 2017) and diazotrophy (Rahav and Bar-Zeev 2017).

Table 2 continued

Phylum	ρ	P value	Change from control to 95%	Change from control to 99%	Change of 95% from 99%	Ecological significance
Proteobacteria	0.22	0.02	N/A	N/A	48.72%	Poorly characterized; initially recovered from marine sediments (Li et al., 1999). Aerobic and mesophilic with some pathogenic; mammalian commensals (Adeolu and Gupta 2013; Garrity et al., 2005). Cosmopolitan aerobes; may restrain other bacterial growth (Aguirre-von-Wobeser et al., 2015)
	– 0.42	< 0.001	– 71.85%	– 96.46%	– 87.43%	Metabolically diverse aerobic chemoorganotrophs; opportunistic pathogens; nosocomial antibiotic resistant strains (Palleroni 1981, Stewart and Costerton 2001, Drenkard and Ausubel 2002). Cosmopolitan aerobes; may restrain other bacterial growth (Aguirre-von-Wobeser et al., 2015)
	– 0.34	< 0.001	– 27.72%	– 69.81%	– 58.23%	Methanotrophs existing where methane and oxygen coexist; can be used as biofilters (Bowman 2014)
	0.4	< 0.001	116.72%	320.90%	94.21%	Typical environmental organisms, plant pathogen; some strains recently identified as human pathogens (LaSala et al., 2007, Mhedbi-Hajri et al., 2011)
	– 0.22	0.02	– 100.00%	– 100.00%	N/A	Aerobic and saccharolytic free-living in soil and nematode symbionts (Janssen and Hedlund 2015).
Verrucomicrobia	– 0.22	0.02	20.82%	– 98.76%	– 98.97%	

Relative abundance of Family-level bacterial OTUs identified by simpler analysis as being significantly affected by treatments within each treatment type. Spearman's ρ and subsequent p value measure the correlation and significance of the correlation of each taxa with treatment intensity (control = 1, 95% = 2, and 99% = 3), while additional columns exhibit the percent change in the relative abundance of taxa in the 95% and 99% treatments from the control, the change in relative abundance of taxa between the 95% and 99% treatments, and some basic ecological information about each taxa listed

2013; Duan & Kaushal, 2015) and by reducing the abundance, diversity, and functional contributions of local populations (Lozupone & Knight 2007; Logares et al., 2009; Dupont et al., 2014). In this study, we demonstrated the effects of elevated salt-related stress on freshwater bacterial communities and we identified several significant characteristics of salt-affected bacterial communities that diverged from control communities. While the relatively narrow focus of this study did not permit us to mechanistically link specific phenomena directly to salt concentrations, we were able to characterize how several pertinent features of bacterial communities are impacted by salt pollution. Together, these findings suggest that freshwater bacterial communities are susceptible to the ever-increasing salinization of freshwater and that this may be detrimental to the capacity of these communities to perform essential ecosystem functions at levels similar to those observed under baseline conditions.

Extracellular enzyme activities are an increasingly effective way to assess microbial functionality as stream microbial populations often require hydrolytic enzymes to catabolize larger molecules so as to gain access to resources, thus enhancing resource cycling within the system (Sabater et al., 2002; Artigas et al., 2015). Due to the immense energy and resource investments required for enzyme synthesis (Koch, 1985), enzyme activity can provide considerable insights into resource acquisition strategies; increasing EEAs are indicative of low resource concentrations or resource demands, while diminished EEA may indicate that resources are readily available and that enzyme production is unnecessary, or that enzyme production may be inhibited by resource deficiencies, or that available resources are being reallocated to other essential activities (Allison and Vitousek, 2005). Salinity has been shown to cause diminished microbial biomass in sediments and soils (Egamberdieva et al., 2010; Tripathi et al., 2018) and although we did not directly measure productivity here, general trends in C and nutrient dynamics can be useful for characterizing community productivity (Frankenberger & Dick, 1983; Hill et al., 2012; Luo et al., 2017).

The diverging LAP and PHOS activities (decreasing and increasing, respectively) in TDS amended communities may simply reflect nutrient acquisition strategies but given the significant reduction in NO_3^- and NH_4^+ concentrations in treated systems, LAP activity would be predicted to increase in response to

diminished nutrient availability, which did not occur. This would suggest that resources remained sufficiently elevated to forego additional enzyme production (Allison and Vitousek, 2005; Vitousek et al., 2010). Examination of vector analyses of enzyme activity ratios suggested that resource limitation—specifically those attributable to P dynamics—may have played a role in observed treatment community EEA (Moorhead et al., 2016). This is somewhat unexpected as several studies have found PHOS EEA to be negatively correlated with salinity concentrations due to the increased availability due to the decrease in P sorption capacity that is commonly associated with brackish or saline waters (Frankenberger & Bingham, 1982; Sundareshwar & Morris, 1999; Pan et al., 2013; Yan et al., 2015). However, when considered within the context of observed LAP EEA, it is perhaps more likely that N concentrations remained elevated enough to inhibit LAP activity while stimulating P acquisition to aid in stoichiometric equilibration and cellular maintenance rather than overt growth (Rose & Axler, 1998; Chen et al., 2019).

Changes in community profiles reflect the taxonomic shifts in community composition that are often observed along freshwater to marine gradients (e.g. reduced abundances of β -Proteobacteria and Actinobacteria taxa—Table 2; Bouvier & del Giorgio, 2002; Telesh & Khlebovich, 2010; Fortunato et al., 2011; Campbell & Kirchman, 2012). This distinction became apparent in α - and β -diversity metrics that consider phylogenetic diversity (e.g., Faith's pd), which likely reflect the genomic transition from less tolerant to more salt-tolerant taxa (Faith & Hawksworth, 1994; Rocca et al., 2020). Moreover, this effect was seen after only a single day of treatment and communities failed to converge over the 9-day experiment, highlighting the sensitivity of the nascent community to salt stress and the rapidity with which freshwater bacterial communities may be affected by continued introduction of salts into the environment (Zhang et al., 2014). Some taxa appeared to be highly sensitive to increasing salinity, resulting in the extirpation of bacteria associated with the metabolically diverse phyla Chloroflexi and the aerobic methane oxidizers of the order Methanococcales (subphylum Gammaproteobacteria) outside of the control communities. However, unique in our data were the response of some taxa (see Table 2) to the induced salinity gradient—specifically in the increase in relative

abundance from the control to 95% treatments and subsequent reduction in relative abundance in the 99% treatments for the same phyla. Abundance of the class Sphingobacteriia (Phylum Bacteroidetes), a strictly aerobic and predominantly saprophytic bacterium, increased by 53% over the control abundances in the 95% treatments before being extirpated from the 99% treatments (Table 2). Similar, albeit less dramatic, results occurred with the phyla Chlorobi and Verrucomirobia, in which significant spikes in relative abundance were observed in the 95% TDS treatments but were not maintained at higher salt concentrations. This suggests there are diverse tolerance thresholds within freshwater communities and that some taxa are capable of surviving increased stress up to a threshold value after which these taxa are negatively affected or lose competitive advantage to more tolerant taxa (Ketola & Hiltunen, 2014). Similar responses have been identified in soil and intertidal sediment communities (Forsyth et al., 1971; Rousk et al., 2011), in which salt-tolerant bacterial populations may not be dominant taxa in situ, but may become increasingly abundant as salinity gradients are introduced. This may explain the significant elevation in the quantities of unique OTUs observed in the 95% treatments, as tolerant OTUs may be beginning to exploit niche space by sensitive taxa that may be approaching extirpation. This may also explain the increase in *nosZ* abundance observed in the TDS treated communities, as the functional plasticity of many denitrifying taxa may promote resilience in the face of altered environmental conditions (Betlach, 1983; Miyahara et al., 2012; Salles et al., 2012) and resource availabilities (Kirchman, 1994; Hoch & Kirchman, 2018).

Conclusion

Salinization of freshwater environments can dramatically affect the structure and functionality of the ecosystem by reducing habitat quality for freshwater organisms and through the modification of resource geochemistry. Understanding how these modifications might affect microbial diversity and microbially mediated biogeochemical processes is a critical first step in identifying ecosystem decline and may provide a means of mitigating these effects prior to further degradation. Projected trends in urban expansion indicate that increased salt strain will unduly fall on

freshwater ecosystems, thus it is imperative to identify how these communities will be impacted. Through an examination of the early successional trajectory of the bacterial community we can gain insights into how affected communities will respond to these types of environmental changes, and whether the structural characteristics or the potential functional capabilities of the microbial community will be maintained in order to assist in mitigating the decline of ecosystem processes. Our findings suggest that while we do see a compositional shift towards a less diverse, albeit what appears to be a more halotolerant, bacterial community, this loss is tempered by the increased potential for N removal via denitrification pathways—a process that is critical to mitigating the negative impacts of nutrient pollution.

Acknowledgements This research has been supported by The Art and Margaret Herrick Aquatic Ecology Research Award, several Kent State University Graduate Student Senate Research Awards and a U.S. Environmental Protection Agency's Science to Achieve Results (STAR) program. This publication was developed under Assistance Agreement No. FP-91781301-0 awarded by the U.S. Environmental Protection Agency to Jonathon B. Van Gray. It has not been formally reviewed by EPA. The views expressed in this document are solely those of J.B. Van Gray, A.A. Roberto, and L.G. Leff and do not necessarily reflect those of the Agency. EPA does not endorse any products or commercial services mentioned in this publication. The authors have no conflict of interests to report.

References

- Aanderud, Z. T., J. C. Vert, J. T. Lennon, T. W. Magnusson, D. P. Breakwell & A. R. Harker, 2016. Bacterial dormancy is more prevalent in freshwater than hypersaline lakes. *Frontiers in Microbiology* 7: 853.
- Allison, S. D. & P. M. Vitousek, 2005. Responses of extracellular enzymes to simple and complex nutrient inputs. *Soil Biology and Biochemistry* 37: 937–944.
- Anderson, M. J., 2001. A new method for non-parametric multivariate analysis of variance. *Austral Ecology* 26: 32–46.
- Anderson, M. J., K. E. Ellingsen & B. H. McArdle, 2006. Multivariate dispersion as a measure of beta diversity. *Ecology Letters* 9: 683–693.
- Araya, R., K. Tani, T. Takagi, N. Yamaguchi & M. Nasu, 2006. Bacterial activity and community composition in stream water and biofilm from an urban river determined by fluorescent in situ hybridization and DGGE analysis. *FEMS Microbiology and Ecology* 43: 111–119.
- Arnon, S., K. A. Gray & A. I. Packman, 2007. Biophysico-chemical process coupling controls nitrogen use by benthic biofilms. *Limnology and Oceanography* 52: 1665–1671.

- Artigas, J., A. M. Romaní & S. Sabater, 2015. Nutrient and enzymatic adaptations of stream biofilms to changes in nitrogen and phosphorus supply. *Aquatic Microbial Ecology* 75: 91–102.
- Baldwin, D. S., G. N. Rees, A. M. Mitchell, G. Watson & J. Williams, 2006. The short-term effects of salinization on anaerobic nutrient cycling and microbial community structure in sediment from a freshwater wetland. *Wetlands* 26: 455–464.
- Bazire, A., F. Diab, M. Jebbar & D. Haras, 2007. Influence of high salinity on biofilm formation and benzoate assimilation by *Pseudomonas aeruginosa*. *Journal of Industrial Microbiology and Biotechnology* 34: 5–8.
- Benjamini, Y. & Y. Hochberg, 1995. Controlling the false discovery rate: a practical and powerful approach to multiple testing. *Journal of the Royal Statistical Society, Series B* 57: 289–300.
- Besemer, K., G. Singer, R. Limberger, A.-K. Chlup, G. Hochedlinger, I. Hödl, et al., 2007. Biophysical controls on community succession in stream biofilms. *Applied and Environmental Microbiology* 73: 4966–4974.
- Betlach, M. R., 1983. Evolution of bacterial denitrification and denitrifier diversity. *Antonie Van Leeuwenhoek* 48: 585–607.
- Bouvier, T. C. & P. A. del Giorgio, 2002. Compositional changes in free-living bacterial communities along a salinity gradient in two temperate estuaries. *Limnology and Oceanography* 47: 453–470.
- Callahan, B. J., P. J. McMurdie, M. J. Rosen, A. W. Han, A. J. A. Johnson & S. P. Holmes, 2016. DADA2: high-resolution sample inference from Illumina amplicon data. *Nature Methods*. <https://doi.org/10.1038/nmeth.3869>.
- Campbell, B. J. & D. L. Kirchman, 2012. Bacterial diversity, community structure and potential growth rates along an estuarine salinity gradient. *International Society of Microbial Ecology Journal* 7: 210.
- Cañedo-Argüelles, M., B. J. Kefford, C. Piscart, N. Prat, R. B. Schäfer & C.-J. Schulz, 2012. Salinisation of rivers: an urgent ecological issue. *Environmental Pollution* 173: 157–167.
- Cañedo-Argüelles, M., C. P. Hawkins, B. J. Kefford, R. B. Schäfer, B. J. Dyack, S. Brucet, et al., 2016. Saving freshwater from salts. *Science* 351: 914–916.
- Caporaso, J. G., J. Kuczynski, J. Stombaugh, K. Bittinger, F. D. Bushman, E. K. Costello, et al., 2010. QIIME allows analysis of high-throughput community sequencing data. *Nature* 7: 335–336.
- Chen, J., J. Seven, T. Zilla, M. A. Dippold, E. Blagodatskaya & Y. Kuzyakov, 2019. Microbial C:N:P stoichiometry and turnover depend on nutrients availability in soil: a ¹⁴C, ¹⁵N, and ³³P triple labelling study. *Soil Biology and Biochemistry* 131: 206–216.
- Clarke, K. R., 1993. Non-parametric multivariate analyses of changes in community structure. *Austral Journal of Ecology* 18: 117–143.
- Corsi, S. R., L. A. De Cicco, M. A. Lutz & R. M. Hirsch, 2015. River chloride trends in snow-affected urban watersheds: increasing concentrations outpace urban growth rate and are common among all seasons. *Science of the Total Environment* 508: 488–497.
- CWT, 2004. Conductivity/salinity measurement principles and methods, DQM IP-3.1.3. In *The Clean Water Team Guidance Compendium for Watershed Monitoring and Assessment, Version 2.0*. Division of Water Quality, California State Water Resources Control Board (SWRCB), Sacramento, CA.
- DeForest, J. L., 2009. The influence of time, storage temperature, and substrate age on potential soil enzyme activity in acidic forest soils using MUB-linked substrates and L-DOPA. *Soil Biology and Biochemistry* 41: 1180–1186.
- Duan, S. & S. S. Kaushal, 2015. Salinization alters fluxes of bioreactive elements from stream ecosystems across land use. *Biogeosciences* 12: 7331.
- Dupont, C. L., J. Larsson, S. Yooseph, K. Ininbergs, J. Goll, J. Asplund-Samuelsson, et al., 2014. Functional tradeoffs underpin salinity-driven divergence in microbial community composition. *Public Library of Science One* 9: 1–9.
- Egamberdieva, D., G. Renella, S. Wirth & R. Islam, 2010. Secondary salinity effects on soil microbial biomass. *Biology and Fertility of Soils* 46: 445–449.
- Evans, D. M., A. M. Villamagna, M. B. Green & J. L. Campbell, 2018. Origins of stream salinization in an upland New England watershed. *Environmental Monitoring and Assessment* 190: 523.
- Faith, D. P. & D. L. Hawksworth, 1994. Phylogenetic pattern and the quantification of organismal biodiversity. *Philosophical Transactions of the Royal Society of London B*. <https://doi.org/10.1098/rstb.1994.0085>.
- Forsyth, M. P., D. B. Shindler, M. B. Gochnauer & D. J. Kushner, 1971. Salt tolerance of intertidal marine bacteria. *Canadian Journal of Microbiology* 17: 825–828.
- Fortunato, C. S., L. Herfort, P. Zuber, A. M. Baptista & B. C. Crump, 2011. Spatial variability overwhelms seasonal patterns in bacterioplankton communities across a river to ocean gradient. *International Society of Microbial Ecology Journal* 6: 554.
- Frankenberger, W. T. & F. T. Bingham, 1982. Influence of salinity on soil enzyme activities. *Soil Science Society of America Journal* 46: 1173–1177.
- Frankenberger, W. T. & W. A. Dick, 1983. Relationships between enzyme activities and microbial growth and activity indices in soil. *Soil Science Society of America Journal* 47: 945–951.
- Franklin, R. B., E. M. Morrissey & J. C. Morina, 2017. Changes in abundance and community structure of nitrate-reducing bacteria along a salinity gradient in tidal wetlands. *Pedobiologia (Jena)*. 60: 21–26.
- Fukami, T. & D. A. Wardle, 2005. Long-term ecological dynamics: reciprocal insights from natural and anthropogenic gradients. *Proceedings of the Royal Society B: Biological Science* 272: 2105–2115.
- Hallin, S., A. Welsh, J. Stenström, S. Hallet, K. Enwall, D. Bru & L. Philippot, 2012. Soil functional operating range linked to microbial biodiversity and community composition using denitrifiers as model guild. *Public Library of Science One* 7: e51962.
- Hart, B. T., P. Bailey, R. Edwards, K. Hortle, K. James, A. McMahon, et al., 1991. A review of the salt sensitivity of the Australian freshwater biota. *Hydrobiologia* 210: 105–144.

- Hill, B. H., C. M. Elonen, L. R. Seifert, A. A. May & E. Tarquinio, 2012. Microbial enzyme stoichiometry and nutrient limitation in US streams and rivers. *Ecological Indicators* 18: 540–551.
- Hintz, W. D. & R. A. Relyea, 2017. Impacts of road deicing salts on the early-life growth and development of a stream salmonid: salt type matters. *Environmental Pollution* 223: 409–415.
- Hoch, M. P. & D. L. Kirchman, 2018. Ammonium uptake by heterotrophic bacteria in the Delaware estuary and adjacent coastal waters. *Limnology and Oceanography* 40: 886–897.
- Hothorn, T., F. Bretz & P. Westfall, 2008. Simultaneous inference in general parametric models. *Biometrical Journal* 50: 346–363.
- Irshad, M., T. Honna, S. Yamamoto, A. E. Eneji & N. Yamasaki, 2005. Nitrogen mineralization under saline conditions. *Communications in Soil Science and Plant Analysis* 36: 1681–1689.
- Jackson, C. R., 2003. Changes in community properties during microbial succession. *Oikos* 101: 444–448.
- Katebian, L. & S. C. Jiang, 2013. Marine bacterial biofilm formation and its responses to periodic hyperosmotic stress on a flat sheet membrane for seawater desalination pretreatment. *Journal of Membrane Science* 425–426: 182–189.
- Katoh, K., K. Misawa, K. Kuma & T. Miyata, 2002. MAFFT: a novel method for rapid multiple sequence alignment based on fast Fourier transform. *Nucleic Acids Research* 30: 3059–3066.
- Kaushal, S. S., P. M. Groffman, G. E. Likens, K. T. Belt, W. P. Stack, V. R. Kelly, et al., 2005. Increased salinization of fresh water in the northeastern United States. *Proceedings of the National Academy of Science* 102: 13517–13520.
- Kaushal, S. S., G. E. Likens, M. L. Pace, R. M. Utz, S. Haq, J. Gorman & M. Grese, 2018. Freshwater salinization syndrome on a continental scale. *Proceedings of the National Academy of Science* 115: E574–E583.
- Ketola, T. & T. Hiltunen, 2014. Rapid evolutionary adaptation to elevated salt concentrations in pathogenic freshwater bacteria *Serratia marcescens*. *Ecology and Evolution* 4: 3901–3908.
- Kim, L. H. & T. H. Chong, 2017. Physiological responses of salinity-stressed *Vibrio* sp. and the effect on the biofilm formation on a nanofiltration membrane. *Environ Science and Technology* 51: 1249–1258.
- Kim, S. & C. Koretsky, 2013. Effects of road salt deicers on sediment biogeochemistry. *Biogeochemistry* 112: 343–358.
- Kirchman, D. L., 1994. The uptake of inorganic nutrients by heterotrophic bacteria. *Microbial Ecology* 28: 255–271.
- Kloos, K., A. Mergel, C. Rösch & H. Bothe, 2001. Denitrification within the genus *Azospirillum* and other associative bacteria. *Functional Plant Biology* 28: 991–998.
- Koch, A. L., 1985. The macroeconomics of microbial growth. In Fletcher, M. & G. D. Floodgate (eds.), *Bacteria in their Natural Environments*. Academic Press, London: 1–42.
- Kunin, V., J. Raes, J. K. Harris, J. R. Spear, J. J. Walker, N. Ivanova, C. von Mering, B. M. Bebout, N. R. Pace, P. Bork & P. Hugenholtz, 2008. Millimeter-scale genetic gradients and community-level molecular convergence in a hypersaline microbial mat. *Molecular Systems Biology*. <https://doi.org/10.1038/msb.2008.35>.
- Lawrence, J. R., G. v D. W. Swerhone, U. Kuhlicke & T. R. Neu, 2007. In situ evidence for microdomains in the polymer matrix of bacterial microcolonies. *Canadian Journal of Microbiology* 53: 450–458.
- Lax, S. & E. W. Peterson, 2009. Characterization of chloride transport in the unsaturated zone near salted road. *Environmental Geology* 58: 1041–1049.
- Lear, G., A. Dopheide, P.-Y. Ancion, K. Roberts, V. Washington, J. Smith & G. D. Lewis, 2012. Biofilms in freshwater: their importance for the maintenance and monitoring of freshwater health. *Current Research Applications, Microbial Biofilms*: 129–151.
- Lenth, R. V., 2016. Least-squares means: the R Package {lsmeans}. *Journal of Statistical Software* 69: 1–33.
- Löfgren, S., 2001. The chemical effects of deicing salt on soil and stream water of five catchments in southeast Sweden. *Water Air and Soil Pollution* 130: 863–868.
- Logares, R., J. Bråte, S. Bertilsson, J. L. Clasen, K. Shalchian-Tabrizi & K. Rengefors, 2009. Infrequent marine–freshwater transitions in the microbial world. *Trends in Microbiology* 17: 414–422.
- Lozupone, C. A. & R. Knight, 2007. Global patterns in bacterial diversity. *Proceedings of the National Academies of Science* 104: 11436–11440.
- Luo, L., H. Meng & J.-D. Gu, 2017. Microbial extracellular enzymes in biogeochemical cycling of ecosystems. *Journal of Environmental Management* 197: 539–549.
- Lycus, P., M. J. Soriano-Laguna, M. Kjos, D. J. Richardson, A. J. Gates, D. A. Milligan, et al., 2018. A bet-hedging strategy for denitrifying bacteria curtails their release of N₂O. *Proceedings of the National Academies of Science* 115: 11820–11825.
- Manz, W., K. Wendt-Potthoff, T. R. Neu, U. Szewzyk & J. R. Lawrence, 1999. Phylogenetic composition, spatial structure, and dynamics of lotic bacterial biofilms investigated by fluorescent in situ hybridization and confocal laser scanning microscopy. *Microbial Ecology* 37: 225–237.
- Miyahara, M., S.-W. Kim, S. Zhou, S. Fushinobu, T. Yamada, W. Ikeda-Ohtsubo, et al., 2012. Survival of the aerobic denitrifier *Pseudomonas stutzeri* strain TR2 during co-culture with activated sludge under denitrifying conditions. *Bioscience, Biotechnology, and Biochemistry* 76: 495–500.
- Moorhead, D. L., R. L. Sinsabaugh, B. H. Hill & M. N. Weintraub, 2016. Vector analysis of ecoenzyme activities reveal constraints on coupled C, N and P dynamics. *Soil Biology and Biochemistry* 93: 1–7.
- Morrissey, E. M. & R. B. Franklin, 2015. Evolutionary history influences the salinity preference of bacterial taxa in wetland soils. *Frontiers in Microbiology* 6: 1013.
- Oksanen, J., Blanchet, F. G., Friendly, M., Kindt, R., Legendre, P., McGlenn, D., et al., 2016. *vegan: community ecology package*.
- Omernik, J. M., 1987. Ecoregions of the conterminous United States. *Annals of the Association of American Geographers* 77: 118–125.
- Oren, A., 1999. Bioenergetic aspects of halophilism. *Microbiology and Molecular Biology Reviews* 63: 334–348.

- Osaka, T., K. Shirota, S. Yoshie & S. Tsuneda, 2008. Effects of carbon source on denitrification efficiency and microbial community structure in a saline wastewater treatment process. *Water Research* 42: 3709–3718.
- Pan, C., C. Liu, H. Zhao & Y. Wang, 2013. Changes of soil physico-chemical properties and enzyme activities in relation to grassland salinization. *European Journal of Soil Biology* 55: 13–19.
- Peck, M., 2012. Middle Cuyahoga River watershed action plan. <http://water.ohiodnr.gov/portals/soilwater/downloads/wap/CuyahogaMiddle.pdf>. Accessed 19 May 2019
- Pinheiro, J., Bates, D., DebRoy, S., Sarkar, D. & R Core Team, 2017. {nlme}: Linear and nonlinear mixed effects models.
- Price, M. N., P. S. Dehal & A. P. Arkin, 2009. FastTree: computing large minimum evolution trees with profiles instead of a distance matrix. *Molecular Biology and Evolution* 26: 1641–1650.
- R Core Team, 2016. R: A language and environment for statistical computing.
- Rath, K. M., A. Maheshwari, P. Bengtson & J. Rousk, 2016. Comparative toxicities of salts on microbial processes in soil. *Applied and Environmental Microbiology* 82: 2012–2020.
- Reed, H. & J. Martiny, 2013. Microbial composition affects the functioning of estuarine sediments. *Journal of the International Society for Microbial Ecology* 7: 868–879.
- Ren, Y., C. Wang, Z. Chen, E. Allan, H. C. van der Mei & H. J. Busscher, 2018. Emergent heterogeneous microenvironments in biofilms: substratum surface heterogeneity and bacterial adhesion force-sensing. *FEMS Microbiology Reviews* 42: 259–272.
- Rietz, D. N. & R. J. Haynes, 2003. Effects of irrigation-induced salinity and sodicity on soil microbial activity. *Soil Biology and Biochemistry* 35: 845–854.
- Ringuelet, S., L. Sassano & Z. I. Johnson, 2011. A suite of microplate reader-based colorimetric methods to quantify ammonium, nitrate, orthophosphate and silicate concentrations for aquatic nutrient monitoring. *Journal of Environmental Monitoring* 13: 370–376.
- Robertson, L. A. & J. G. Kuenen, 1984. Aerobic denitrification—old wine in new bottles? *Antonie Van Leeuwenhoek* 50: 525–544.
- Rocca, J. D., M. Simonin, E. S. Bernhardt, A. D. Washburne & J. P. Wright, 2020. Rare microbial taxa emerge when communities collide: freshwater and marine microbiome responses to experimental mixing. *Ecology* 101: e02956.
- Rose, C. & R. P. Axler, 1998. Use of alkaline phosphatase activity in evaluating phytoplankton community phosphorus deficiency. *Hydrobiologia* 361: 145–156.
- Rousk, J., F. K. Elyaagubi, D. L. Jones & D. L. Godbold, 2011. Bacterial salt tolerance is unrelated to soil salinity across an arid agroecosystem salinity gradient. *Soil Biology and Biochemistry* 43: 1881–1887.
- Roy, J. W., R. McInnis, G. Bickerton & P. L. Gillis, 2015. Assessing potential toxicity of chloride-affected groundwater discharging to an urban stream using juvenile freshwater mussels (*Lampsilis siliquoidea*). *Science of the Total Environment* 532: 309–315.
- Sabater, S., H. Guasch, A. Romaní & I. Muñoz, 2002. The effect of biological factors on the efficiency of river biofilms in improving water quality. *Hydrobiologia* 469: 149–156.
- Salles, J. F., X. Le Roux & F. Poly, 2012. Relating phylogenetic and functional diversity among denitrifiers and quantifying their capacity to predict community functioning. *Frontiers in Microbiology* 3: 209.
- Samuels, C. L. & J. A. Drake, 1997. Divergent perspectives on community convergence. *Trends in Ecology and Evolution* 12: 427–432.
- Schuler, M. S., W. D. Hintz, D. K. Jones, L. A. Lind, B. M. Mattes, A. B. Stoler, et al., 2017. How common road salts and organic additives alter freshwater food webs: in search of safer alternatives. *Journal of Applied Ecology* 54: 1353–1361.
- Setzinger, S. P., W. S. Gardner & A. K. Spratt, 1991. The effect of salinity on ammonium sorption in aquatic sediments: implications for benthic nutrient recycling. *Estuaries* 14: 167–174.
- Sévin, D. C., J. N. Stählin, G. R. Pollak, A. Kuehne & U. Sauer, 2016. Global metabolic responses to salt stress in fifteen species. *Public Library of Science One* 11: e0148888–e0148888.
- Servais, S., J. S. Kominoski, S. P. Charles, E. E. Gaiser, V. Mazzei, T. G. Troxler & B. J. Wilson, 2019. Saltwater intrusion and soil carbon loss: testing effects of salinity and phosphorus loading on microbial functions in experimental freshwater wetlands. *Geoderma* 337: 1291–1300.
- Singer, G., K. Besemer, I. Hödl, A. K. Chlup, G. Hochedlinger, P. Stadler & T. J. Battin, 2006. Microcosm design and evaluation to study stream microbial biofilms. *Limnology and Oceanography: Methods* 4: 436–447.
- Sleator, R. D. & C. Hill, 2002. Bacterial osmoadaptation: the role of osmolytes in bacterial stress and virulence. *FEMS Microbiology Reviews* 26: 49–71.
- Smucker, N. J., J. L. DeForest & M. L. Vis, 2009. Different methods and storage duration affect measurements of epilithic extracellular enzyme activities in lotic biofilms. *Hydrobiologia* 636: 153–162.
- Stoodley, P., K. Sauer, D. G. Davies & J. W. Costerton, 2002. Biofilms as complex differentiated communities. *Annual Review of Microbiology* 56: 187–209.
- Strahler, A. N., 1964. Quantitative geomorphology of drainage basins and channel networks. In Chow, V. T. (ed.), *Handbook of applied hydrology*. McGraw-Hill, New York: 439–476.
- Sundareshwar, P. V. & J. T. Morris, 1999. Phosphorus sorption characteristics of intertidal marsh sediments along an estuary salinity gradient. *Limnology and Oceanography* 44: 1693–1701.
- Telesh, I. V. & V. V. Khlebovich, 2010. Principal processes within the estuarine salinity gradient: a review. *Marine Pollution Bulletin* 61: 149–155.
- Throbäck, I. N., K. Enwall, Å. Jarvis & S. Hallin, 2004. Reassessing PCR primers targeting nirS, nirK and nosZ genes for community surveys of denitrifying bacteria with DGGE. *FEMS Microbiology Ecology* 49: 401–417.
- Tolker-Nielsen, T. & S. Molin, 2000. Spatial organization of microbial biofilm communities. *Microbial Ecology* 40: 75–84.
- Tripathi, B. M., J. C. Stegen, M. Kim, K. Dong, J. M. Adams & Y. K. Lee, 2018. Soil pH mediates the balance between stochastic and deterministic assembly of bacteria. *Journal*

- of the International Society of Microbial Ecology. <https://doi.org/10.1038/s41396-018-0082-4>.
- Turner, S., K. M. Pryer, V. P. W. Miao & J. D. Palmer, 1999. Investigating deep phylogenetic relationships among cyanobacteria and plastids by small subunit rRNA sequence analysis. *Journal of Eukaryotic Microbiology* 46: 327–338.
- Vitousek, P. M., S. Porder, B. Z. Houlton & O. A. Chadwick, 2010. Terrestrial phosphorus limitation: mechanisms, implications, and nitrogen-phosphorus interactions. *Ecological Applications* 20: 5–15.
- Wang, H., J. A. Gilbert, Y. Zhu & X. Yang, 2018. Salinity is a key factor driving the nitrogen cycling in the mangrove sediment. *Science of the Total Environment* 631–632: 1342–1349.
- Weston, N. B., R. E. Dixon & S. B. Joye, 2006. Ramifications of increased salinity in tidal freshwater sediments: Geochemistry and microbial pathways of organic matter mineralization. *Journal of Geophysical Research Biogeosciences*. <https://doi.org/10.1029/2005JG000071>.
- Williams, W. D., 2001. Anthropogenic salinisation of inland waters. *Hydrobiologia* 466: 329–337.
- Yan, N., P. Marschner, W. Cao, C. Zuo & W. Qin, 2015. Influence of salinity and water content on soil microorganisms. *International Soil and Water Conservation Research* 3: 316–323.
- Zhang, H., 2004. The optimality of naive Bayes. In *Proceedings of the 17th International Florida Artificial Intelligence Research Society Conference*, AAAI Press, pp 562–567
- Zhang, L., G. Gao, X. Tang & K. Shao, 2014. Can the freshwater bacterial communities shift to the “marine-like” taxa? *Journal of Basic Microbiology* 54: 1264–1272.
- Zwart, G., B. C. Crump, M. P. K. Agterveld & F. Hagen, 2002. Typical freshwater bacteria: an analysis of available 16S rRNA gene sequences from plankton of lakes and rivers. *Aquatic Microbial Ecology* 28: 141–155.

Publisher's Note Springer Nature remains neutral with regard to jurisdictional claims in published maps and institutional affiliations.